Med & Health Mar 2024; 19(1): 204-219 https://doi.org/10.17576/MH.2024.1901.14

ORIGINAL ARTICLE

Metabolic Profiling Reveals the Importance of Arginine Metabolism via the Arginine Deiminase Pathway in Vancomycin-intermediate *S. aureus*

TAN JK[1], TAN XE[2], NEOH HM[3]*

[1]*Department of Biochemistry, Faculty of Medicine, Universiti Kebangsaaan Malaysia, Jalan Yaacob Latiff, Bandar Tun Razak, 56000 Cheras, Kuala Lumpur, Malaysia*
[2]*Department of Infection and Immunity, School of Medicine, Jichi Medical University, 329-0498 Japan*
[3]*UKM Molecular Medical Biology Institute (UMBI), Universiti Kebangsaaan Malaysia, Jalan Yaacob Latiff, Bandar Tun Razak, 56000 Cheras, Kuala Lumpur, Malaysia*

Received: 19 Oct 2023 / Accepted: 28 Nov 2023

ABSTRAK

Mutasi gen dalam VraSR dan GraSR, dua sistem pengawalseliaan dua komponen telah dilaporkan menyebabkan rintangan vankomisin dalam Staphylococcus aureus berkerintangan perantaraan vankomisin (VISA). Pemprofilan proteomik perbandingan antara S. aureus rentan vankomisin (VSSA) dan Staphylococcus aureus rintang vankomisin (VISA) daripada keturunan genetik Mu50 mendedahkan pengekspresan yang meningkat untuk protein katabolik ornithine carbamoyltransferase (ArcB); ini mencadangkan peranan katabolisme arginin dalam pembentukan VISA. Kajian ini bertujuan untuk menyiasat dengan lebih lanjut tapak laluan metabolik yang berkaitan dengan pembentukan VISA menggunakan pemprofilan metabolomik tidak bersasar berasaskan "liquid chromatography mass spectrometry" (LCMS). Profil metabolit antara 3 strain isogenik keturunan Mu50 iaitu Mu50 (VSSA), Mu50 -vraSm (VISA) dan Mu50 -vraSm-graRm (VISA) telah dibanding. Paras intrasel bagi asid α-hidroksiglutarik, kolin, lisin, asid malik, N-asetilornithine, nikotinamida dan cystathionine didapati berbeza dengan ketara antara VISA berbanding VSSA. Sel VISA didapati mempunyai tahap citrulline intraselular dan arginin ekstraselular yang lebih rendah, dengan tahap ornithine ekstraselular yang lebih tinggi berbanding VSSA. Perbezaan tahap metabolit antara VISA dan VSSA ini mencadangkan kepentingan metabolisme arginine dalam kerintangan perantaraan kepada vankomisin. Pengaktifan tapak laluan arginine deiminase (ADI) dalam VISA dari keturunan Mu50 boleh diterokai lebih lanjut

Address for correspondence and reprint requests: Hui-min Neoh. UKM Medical Molecular Biology Institute (UMBI), Universiti Kebangsaan Malaysia, Jalan Yaacob Latif, 56000 Cheras, Kuala Lumpur, Malaysia. Tel: +603-9145-9074 Email: hui-min@ppukm.ukm.edu.my

sebagai sasaran untuk pembangunan antibiotik.

Kata kunci: Metabolomik; Staphylococcus aureus berkerintangan-perantaraan vankomisin (VISA); tapak laluan arginine deiminase (ADI)

ABSTRACT

Gene mutations located in VraSR and GraSR, two-component regulatory systems have been reported to cause vancomycin resistance in vancomycin-intermediate *Staphylococcus aureus* (VISA). Subsequent comparative proteomic profiling between vancomycin-susceptible *S. aureus* (VSSA) and VISAs of the Mu50 genetic lineage revealed up-regulated level of catabolic ornithine carbamoyltransferase (ArcB) in the latter, suggesting a role of arginine catabolism in VISA development. This study aimed to further investigate metabolic pathways associated with VISA development using liquid chromatography mass spectrometry (LCMS)-based untargeted metabolomic profiling. Metabolite profiles were compared among 3 isogenic strains of the Mu50 lineage: Mu50Ω (VSSA), Mu50Ω-vraSm (VISA) and Mu50Ω-vraSm-graRm (VISA). Intracellular levels of α-hydroxyglutaric acid, choline, lysine, malic acid, N-acetylornithine, nicotinamide, and cystathionine were found to be significantly different between VISAs compared to VSSA. VISA cells were found to have lower levels of intracellular citrulline and extracellular arginine, with higher extracellular level of ornithine compared to VSSA. These differences in metabolite levels between VISA and VSSA suggested the importance of arginine metabolism. Activation of the arginine deiminase pathway (ADI) in VISAs of the Mu50 lineage could be further explored as a target for antibiotic development.

Keywords: Arginine deiminase (ADI) pathway; metabolomics; vancomycin-intermediate *S. aureus* (VISA)

INTRODUCTION

Staphylococcus aureus is a commensal bacterium that can turn into an opportunistic pathogen and cause life-threatening infections (McGuinness et al. 2017). The global dissemination of methicillin-resistant *S. aureus* (MRSA) strains, lead to the widespread usage of vancomycin, a glycopeptide, to treat MRSA infections. This selection pressure has led to the emergence and dissemination of the vancomycin-intermediate *S. aureus* (VISA; vancomycin minimum inhibitory concentration, MIC ≥4 mg/L) (Hiramatsu et al. 2014). These strains differ from vancomycin-resistant *S. aureus* (VRSA) (vancomycin MIC ≥16 mg/L), where the mechanism of resistance in VRSA has been attributed to acquisition of the enterococcal *vanA* operon (Weigel et al. 2003). The development of VISA is not well

understood, but is thought to be related to the acquisition of mutations in resistant-related genes including *walKR, vraSR* and *graSR*, all of which are involved in cell wall synthesis (McGuinness et al. 2017). Although varied in genotypes, most VISA strains display thick cell walls, reduction in autolytic activity and altered growth rates (Koehl et al. 2004; McCallum et al. 2006; Tan et al. 2017).

Vancomycin resistance-associated sensor/regulator (VraSR) and glycopeptide-resistance-associated sensor/regulator (GraSR) are members of two two-component regulatory systems involved in cell wall synthesis (Kuroda et al. 2003; McGuinness et al. 2017; Neoh et al. 2008). Strains carrying mutations that activate VraSR and GraSR are reported to have reduced vancomycin susceptibility. However, the exact mechanism of VISA transformation regulated by these systems remains unknown (Cui et al. 2009). In a previous study, both VISAs Mu50Ω-*vraS*m and Mu50Ω-*vraS*m-*graR*m were genetically engineered from Mu50Ω, a vancomycin-susceptible *S. aureus* (VSSA) isolated from the same patient as Mu50 (the first reported clinical isolate of VISA). These strains were intended to mirror the transformation of VSSA to VISA in Mu50-like strains through VraSR and GraSR regulons (Hiramatsu et al. 1997; Cui et al. 2009). Mu50Ω-*vraS*m carries a *vraS* T700A mutation (methionine-234 to stop codon), whereas Mu50Ω-*vraS*m-*graR*m harbours both *vraS* T700A and *graR* A590G mutations (asparagine-197 to serine) (Figure 1). Mu50Ω, Mu50Ω-*vraS*m and Mu50Ω-*vraS*m-*graR*m are isogenic strains. They are ascending in the order of their vancomycin resistance, with vancomycin MIC values of 0.5, 4.5 and 6 mg/L, respectively. Our subsequent proteomic analysis reported on the up-regulation of several proteins associated with information processing, signalling and metabolism in these VISAs. In particular, catabolic ornithine carbamoyltransferase (ArcB), a structural gene in the arginine deiminase (ADI) pathway, was found to be consistently overexpressed in both Mu50Ω-*vraS*m and Mu50Ω-

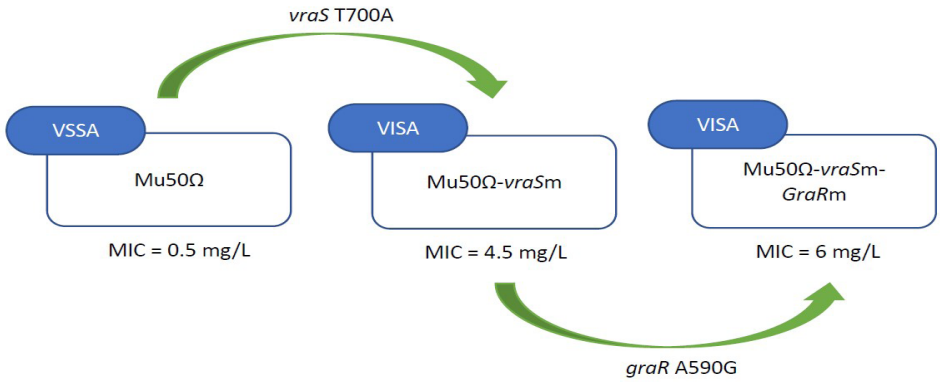

FIGURE 1: Stepwise transformation of VISA from VSSA in Mu50 line-age through VraSR and GraSR regulons

*vraS*m-*graR*m strains (Tan et al. 2016), hinting at a possible role for arginine metabolism in VISA development.

The metabolome reflects the physiological status of an organism, and study of the metabolome can used to understand mechanisms involved in changes in an organism in response to environmental stimuli. Previous studies employing metabolomics reported that a number of metabolic pathways including cell wall metabolism, the pentose phosphate pathway and the tricarboxylic acid cycle were associated with the VISA phenotype (Alexander et al. 2014; Gardner et al. 2018; Hattangady et al. 2015). However, the VISAs tested in these studies harboured mutations in places besides VraSR and GraSR regions, and the VISAs were not from the Mu50 lineage. In the present study, we used liquid chromatography mass spectrometry (LCMS)-based untargeted metabolomic profiling to investigate metabolic changes associated with VraSR and GraSR mutations in VISAs of the Mu50 lineage.

MATERIALS AND METHODS

Sample Collection

The three isogenic *S. aureus* strains Mu50Ω, Mu50Ω-*vraS*m and Mu50Ω-*vraS*m-*graR*m used in this study were generated in a previous study (Cui et al. 2009). The strains were cultured overnight in Brain Heart Infusion broth (Becton Dickinson, Franklin Lakes, NJ, USA) at 37˚C. Cell numbers were counted and 1 mL of cells from each tested strain was collected by centrifugation at 12,000 rpm for 2 minutes at 16˚C. The supernatant (medium) was transferred to a new tube and used for extracellular metabolome analysis. Cell pellets were washed three times with 1 mL NaCl (0.9%), and subsequently centrifuged for 2 minutes at 12,000 rpm, 16˚C, and used for intra-cellular metabolome analysis. Each group consisted of three biological replicates.

Metabolite Extraction

All chemicals used were of mass spectrometry-grade (Fisher Scientific, Waltham, MA, USA). The metabolite extraction protocol was modified from previous studies (Dunn et al. 2011; Liebeke et al. 2010). A total of 800 µL cold methanol (60%) was added to the cell pellet. The solution was then vortexed for 15 seconds and homogenised with a probe sonicator (20 amplitude, 10 seconds, three times; Qsonica, Newtown, CT, USA). Prior to the extraction of metabolites from medium samples, a quality control (QC) sample for medium samples was prepared by aliquoting 40 µL from each sample into a pool and extracting as medium samples. A total of 800 µL cold methanol (100%) was added to the 200 µL medium sample and vortexed for 15 seconds. Cell and medium samples were centrifuged at 16,000 g for 15 minutes at 4˚C. The supernatant was then transferred to a fresh tube and dried using a vacuum concentrator at room temperature (Eppendorf, Hamburg, Germany). The dried pellet was kept at 80˚C until further use.

Liquid Chromatography Mass Spectrometry (LCMS)

Cell and medium samples were reconstituted in 200 µL water for every 1 x 10^6 cells. The solution was then and filtered through a 0.2 µm regenerated cellulose membrane (Thermo Scientific, Waltham, MA, USA). The QC sample was prepared combining aliquots of 10 µL extracts from each cell sample. Liquid chromatography (LC) was carried out using Dionex Ultimate 3000 UHPLC coupled to Q Exactive HF Orbitrap MS/MS (Thermo Scientific) via a heated electrospray ionisation (ESI) probe. The system was calibrated with Pierce ESI ion calibration solutions (Thermo Scientific). A C18 column (1.7 µm x 2.1 mm x 100 mm; Synchronis; Thermo Scientific) was used for LC. A 2 µL sample was injected through a heated column at 55˚C with a 450 µL/min flow rate. A 22 minutes elution gradient using mobile phase A (water with 0.1% formic acid) and B (acetonitrile with 0.1% formic acid) was performed by using 0.5% B for 1 minute, 0.5%–99.5% B for 15 minutes, 99.5% B for 4 minutes and 0.5% B for 2 minutes. A full MS scan ranging from 100-1,000 *m/z* at 60,000 resolution was collected, whereas an MS/MS scan was collected at a resolution of 15,000. Negative ion mode was performed after the completion of positive ion mode (Tan et al. 2023).

Data Analysis

Data were pre-processed using Compound Discoverer 2.0 (Thermo Scientific). Briefly, peaks were aligned within 5 ppm, background subtracted using water as a blank sample and annotated using the mzClound database (HighChem LLC, Slovakia). Molecular features (MFs) of retention time, molecular weight and peak intensity were extracted for statistical analysis. Significantly different MFs between groups were identified using MetaboAnalyst 4.0 (Chong et al. 2018). Briefly, MFs were grouped at 0.025 *m/z* and 30 seconds retention time, filtered using inter-quartile range, log transformed and auto scaled. Multivariate analyses were performed using Principle Component Analysis (PCA) and Partial Least Squares-Discriminant Analysis (PLS-DA), whereas univariate analysis was carried out using ANOVA with Fisher's LSD as post-hoc test. Unless specified, a false discovery rate (FDR) <0.05 was considered statistically significant for all tests. The QC coefficient of variation (CV) filtering was set at <30%, unless specified otherwise. Pathway analysis of significantly different metabolites was performed using MetaboAnalyst 4.0. A hypergeometric test was used for over representative analysis, relative-betweenness centrality was used for pathway topology analysis and the pathway library was mapped to *S. aureus* N315 (KEGG) (Kanehisa 2019).

Metabolite Annotation

Significantly different MFs were annotated via matching of the MFs' accurate mass and MS/MS spectrum to online libraries, namely mzCloud, Human Metabolome Database

(HMDB) (Wishart et al. 2018) and METLIN (Guijas et al. 2018). First, annotation based on mzCloud was performed automatically by Compound Discoverer. Then, the remaining significantly different MFs were searched against CEU Mass Mediator (Gil-De-La-Fuente et al. 2019) which linked to HMDB and METLIN for mass matching. The MFs with matched mass were further searched in HMDB and METLIN databases for MS/MS spectral matching at an MS/MS tolerance of <0.01 Da. Only MFs with a level 2 confidence annotation (Sumner et al. 2007) were reported in this study and determined to be metabolites. Level 2 confidence annotation was defined in this study as a putative annotation for a compound with matched mass (<5 ppm) and MS/MS spectrum (>70%) to the databases.

RESULTS

Distribution of Samples

QC samples were identified to be clustered together in the PCA score plot, indicating stable performance of the instrument (Figure 2). There was an overlap of the Mu50Ω-*vraS*m intra-

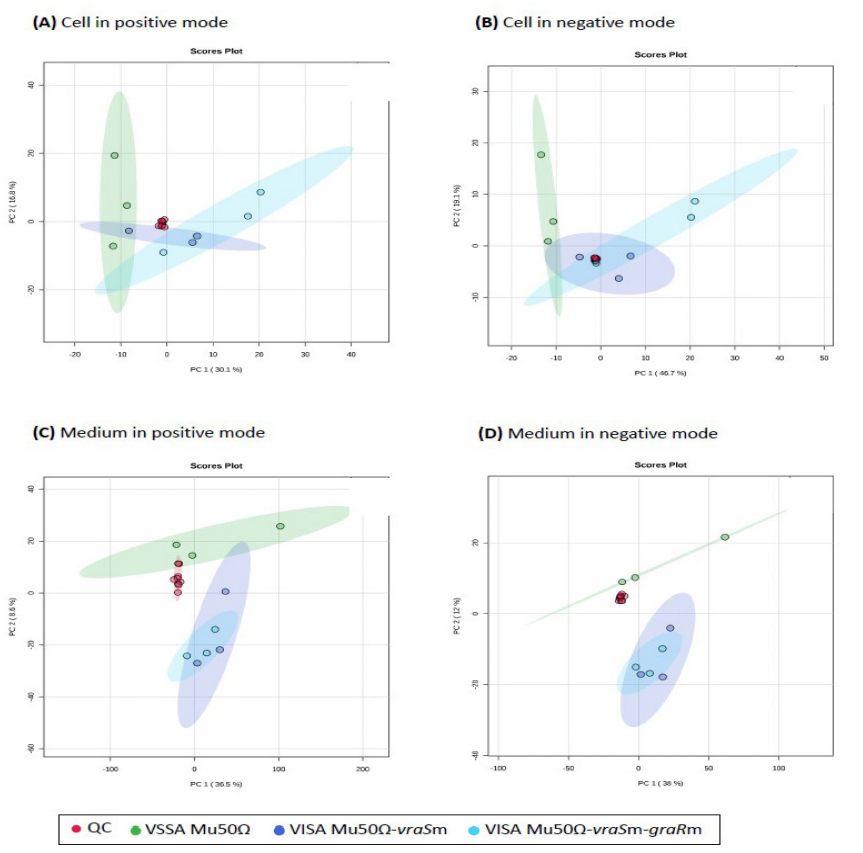

FIGURE 2: Distribution of QCs in PCA score plot; (A & B) Cell and (C &D) medium in positive and negative ion modes, respectively

cellular metabolome with the intracellular metabolomes of Mu50Ω and Mu50Ω-*vraS*m-*graR*m, suggesting a correlation between cells' vancomycin MIC levels and their metabolic changes (Figure 3). The extracellular metabolomes of Mu50Ω-*vraS*m and Mu50Ω-*vraS*m-*graR*m overlapped with each other, but they were separate from Mu50Ω. This data suggested a similar metabolite composition in the media of both VISAs that differed from the metabolite composition in the VSSA media. While these observations were visualised from the PLS-DA score plot, permutation tests were not significant and Q2 values were < 80% (Figure 4). Therefore, a univariate ANOVA was used for further analysis.

Number of Significantly Different Intra-cellular Metabolites

A total of 286 and 189 intra-cellular MFs were detected in positive and negative ion modes, respectively (Table 1). Comparison of the metabolomes of Mu50Ω-*vraS*m and Mu50Ω revealed 11 (3.8%, positive ion mode) and 14 (7.4%, negative ion mode) significantly

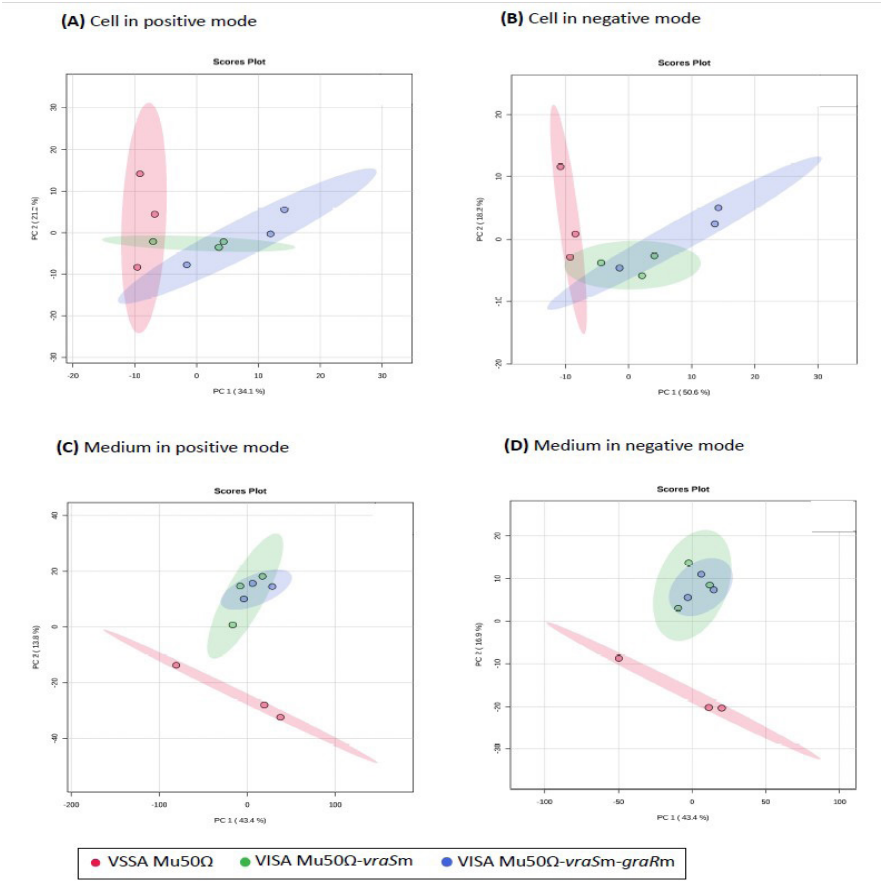

FIGURE 3: Distribution of samples in PCA score plot; (A & B) Cell and (C &D) medium in positive and negative ion modes, respectively

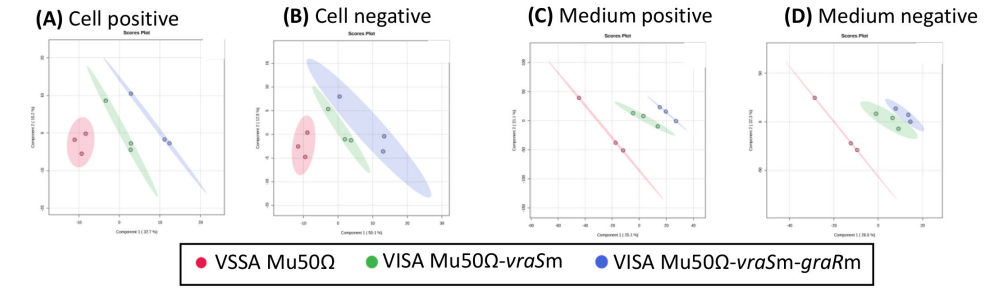

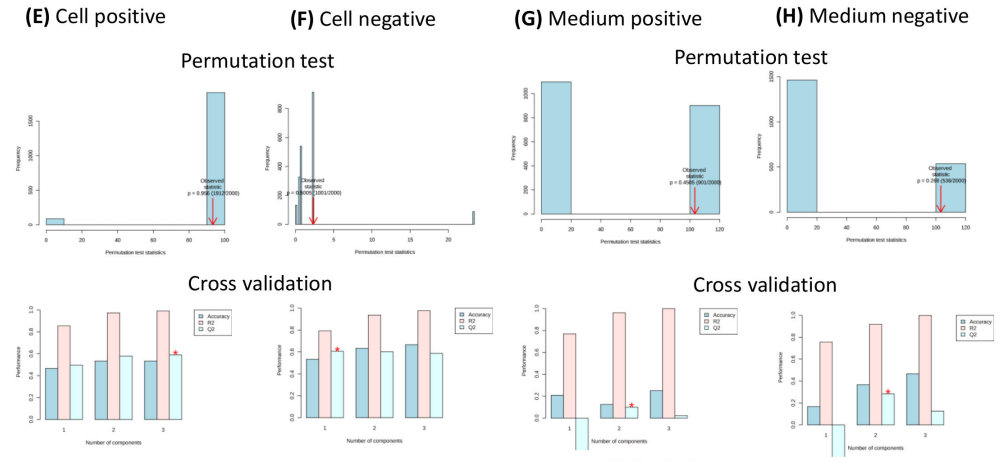

PLS-DA cross validation details:

Measure	1 comps	2 comps	3 comps*
Accuracy	0.46667	0.53333	0.53333
R2	0.85497	0.97393	0.99096
Q2	0.49579	0.57936	0.5907

PLS-DA cross validation details:

Measure	1 comps*	2 comps	3 comps
Accuracy	0.53333	0.63333	0.66667
R2	0.79281	0.93678	0.97655
Q2	0.60608	0.60275	0.58669

PLS-DA cross validation details:

Measure	1 comps	2 comps*	3 comps
Accuracy	0.20833	0.125	0.25
R2	0.76967	0.9624	0.99966
Q2	-0.53121	0.10007	0.02326

PLS-DA cross validation details:

Measure	1 comps	2 comps*	3 comps
Accuracy	0.16667	0.36667	0.46667
R2	0.75656	0.91811	0.99889
Q2	-0.29516	0.2837	0.12572

FIGURE 4: PLS-DA of samples. Score plot of (A & B) Cell and (C &D) medium in positive and negative ion modes, respectively. Permutation test and cross validation of (E & F) cell and (G &H) medium in positive and negative ion modes, respectively

different MFs between the two strains. However, only 4/11 (36.4%, positive ion mode) and 3/14 (14.3%, negative ion mode) of these were annotated. We observed the same number for the difference in metabolomes between Mu50Ω-*vraS*m-*graR*m and Mu50Ω. For comparison of the metabolomes between Mu50Ω-*vraS*m-*graR*m and Mu50Ω-*vraS*m, only 2/286 (0.7%, positive ion mode) and 1/198 (0.5%, negative ion mode) MFs were significantly different, but none of these were annotated.

Number of Significantly Different Extracellular Metabolites

For the extracellular metabolome represented by metabolites in culture medium, a total of 4672 and 1579 MFs were found to be in positive and

TABLE 1: Number of total, significantly different and annotated MFs.

	Cell						Medium					
	Mu50Ω-*vraS*m vs Mu50Ω		Mu50Ω-*vraS*m-*graR*m vs Mu50Ω		Mu50Ω-*vraS*m-*graR*m vs Mu50Ω-*vraS*m		Mu50Ω-*vraS*m vs Mu50Ω		Mu50Ω-*vraS*m-*graR*m vs Mu50Ω		Mu50Ω-*vraS*m-*graR*m vs Mu50Ω-*vraS*m	
Ion mode	+	-	+	-	+	-	+	-	+	-	+	-
Total of MFs detected	286	189	286	189	286	189	4672	1579	4672	1579	4672	1579
Significantly different MFs	11	14	11	14	2	1	1	0	1	0	0	0
Significantly different metabolites (annotated)*	4	3	4	3	0	0	0	0	0	0	0	0
Total of significantly different metabolites with QC CV < 30%	6		6		0		0		0		0	

MFs: metabolite features; *only metabolites with level 2 confidence annotation were included; QC CV: coefficient of variation for QC samples

negative ion modes, respectively (Table 1). However, only 1/4672 (0.02%) MF in positive mode was found to be significantly different between Mu50Ω-*vraS*m and Mu50Ω, and between Mu50Ω-*vraS*m-*graR*m and Mu50Ω. However, this MF was not annotated. No significant differences in MFs were detected between Mu50Ω-*vraS*m-*graR*m and Mu50Ω-*vraS*m.

Identification of Significantly Different Metabolites

Intra-cellular levels of α-hydroxyglutaric acid, choline (QC CV=34.4%), lysine, malic acid, N-acetylornithine and nicotinamide were found to be higher in the VISA strains compared to VSSA, whereas intra-cellular cystathionine levels were lower (Table 2; Figure 5). These metabolites were matched to metabolic pathways including cysteine and methionine metabolism, lysine biosynthesis and arginine biosynthesis (Table 3). However, because only one to two of these metabolites were matched to each pathway, further investigation is required to determine whether the associated pathways are important in VISAs or if the pathways are activated only when cells come into contact with vancomycin.

We detected other metabolites associated with arginine metabolism in this study, namely citrulline, aspartic acid, arginine, ornithine and N-acetylglutamic acid. Although not statistically significant, intra-cellular citrulline levels were lower in VISA strains compared to the VSSA strain (Figure 6). Similarly, aspartic acid and arginine levels were lower in VISA

TABLE 2: List of significantly different intracellular metabolites in Mu50Ω-vraSm and Mu50Ω-vraSm-graRm

Compound Name	HMDB ID	Ionization Mode
Up regulated*		
α-Hydroxyglutaric acid	HMDB0059655	-
Choline (QC CV = 34.4%)	HMDB0000097	+
Lysine	HMDB0000182	+
Malic acid	HMDB0000156	-
N-acetylornithine	HMDB0003357	+
Nicotinamide	HMDB0001406	+
Down regulated*		
Cystathionine	HMDB0000099	-

*compared with Mu50Ω; all metabolites with QC CV (quality control coefficient of variation) < 30% unless specified otherwise; "+": positive ion mode; "-": negative ion mode; HMDB: human metabolome database

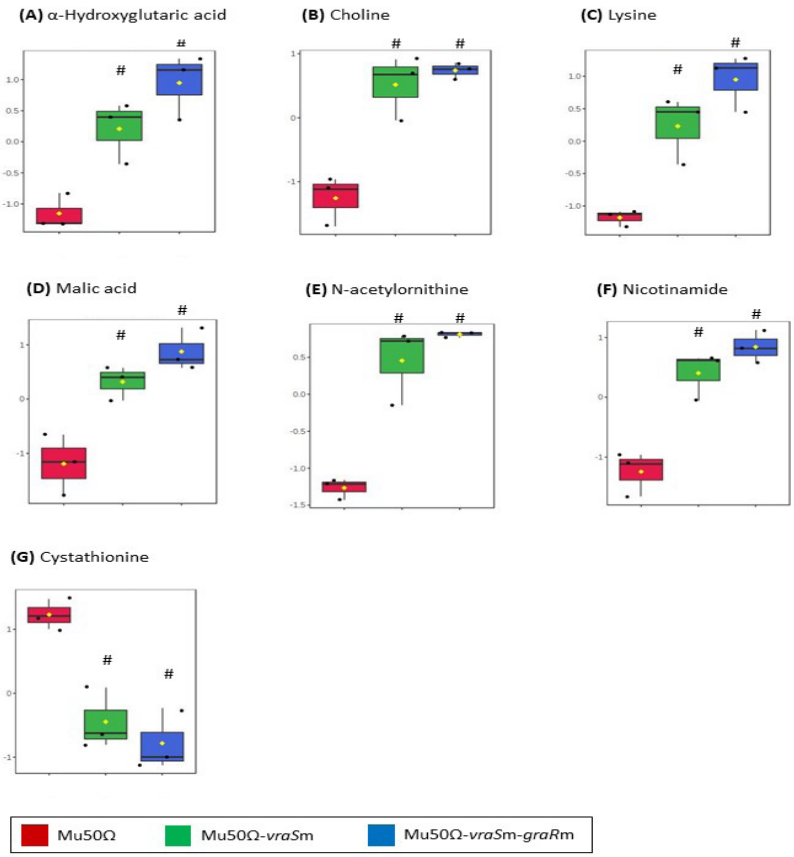

FIGURE 5: Boxplot of significantly different metabolites annotated in the cells; (A) α-Hydroxyglutaric acid; (B) choline; (C) lysine; (D) malic acid; (E) N-acetylornithine; (F) nicotinamide; and (G) cystathionine. N=3; ANOVA with Fisher's LSD post-hoc test; #significantly different from Mu50Ω, FDR <0.05; Y-axis: normalised concentration

TABLE 3: Pathway analysis

Pathway Name	Match Metabolites/ total in pathway	p	FDR	Impact
Glycine, serine and threonine metabolism	2/29: choline, cystathionine	0.025 0.078	1.0 1.0	0.00 0.00
Nicotinate and nicotinamide metabolism	1/9: nicotinamide	0.119	1.0	0.00
Lysine biosynthesis	1/14: lysine	0.135	1.0	0.00
Arginine biosynthesis	1/16: N-acetylornithine			
Glycerophospholipid metabolism	1/16: choline	0.135	1.0	0.00
Cysteine and methionine metabolism	1/30: cystathionine	0.240	1.0	0.18
Aminoacyl-tRNA biosynthesis	1/45: lysine	0.340	1.0	0.00

strains, whereas N-acetylglutamic acid and ornithine (QC CV=55.2%) levels were higher in the culture media of VISAs.

DISCUSSION

Cell wall thickening is crucial for the VISA phenotype because it protects peptidoglycan synthesis in the cytoplasmic membrane by trapping and clogging vancomycin in outer cell wall layers (Cui et al. 2005). Therefore, metabolic changes in VISA development driven by mutations in v*raSR* and *graSR* are conceivably closely related to cell wall metabolism, as these two regulatory systems are involved in cell wall synthesis (Cui et al. 2009; Kuroda et al. 2003; Neoh et al. 2008). However, metabolic pathways mediated by mutations in *vraSR* and *graSR* in VISA to achieve vancomycin-intermediate resistance are largely unknown and were the topic of investigation in this study.

We took a metabolomics approach and found that levels of several metabolites, including α-hydroxyglutaric acid, choline, lysine, malic acid, N-acetylornithine, nicotinamide and cystathionine, were altered in VISA cells. These metabolites may be primarily regulated by VraSR because the concentrations of these metabolites were not significantly different between Mu50Ω-*vraS*m and Mu50Ω-*vraS*m-*graR*m. However, as these metabolite levels were in accordance with the vancomycin MIC values of our tested strains, the *graR* A590G mutation may have further augmented metabolic processes related to these metabolites to lower vancomycin susceptibility.

Although not statistically significant, we found altered levels of metabolites associated with arginine metabolism in VISA cells. Interestingly, this finding agreed with the results of our differential proteomic profiling of the three strains tested, where higher expression of the catabolic ArcB protein in both Mu50Ω-*vraS*m and Mu50Ω-*vraS*m-*graR*m indicated arginine catabolism (Tan et al. 2016). ArcB is a structural gene of the ADI pathway, which catabolises arginine to ornithine, ammonia, carbon dioxide and ATP (Lindgren et al. 2014). We hypothesised that the reduction of arginine in the culture media of VISAs in our study can be attributed

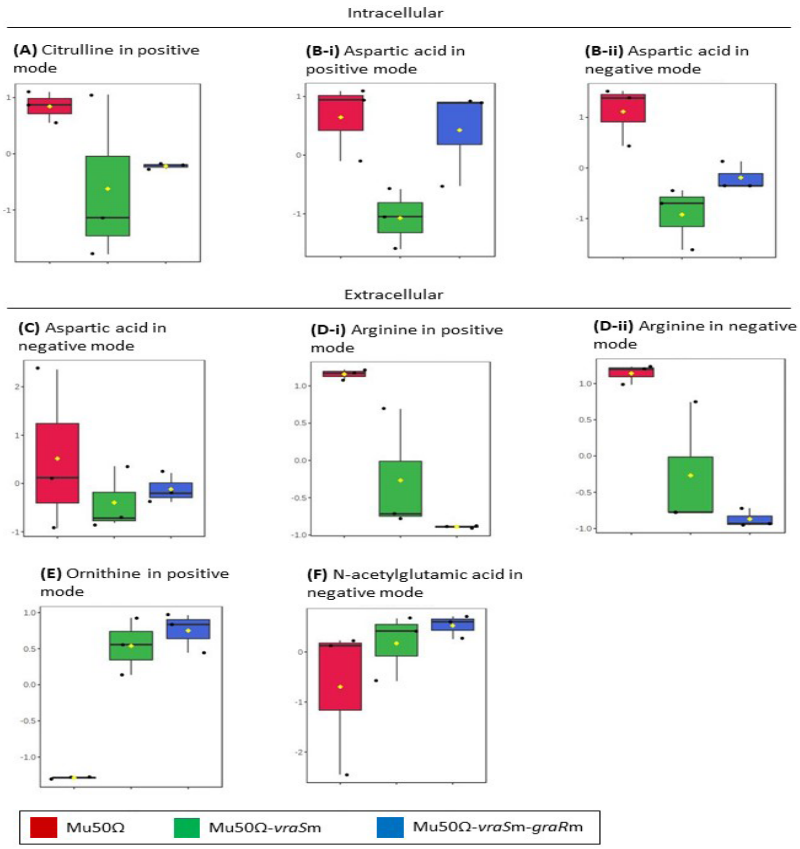

FIGURE 6: Boxplot of other arginine metabolism-related metabolites detected in this study; (A) Citrulline and (B) aspartic acid were found in the cell; (C) Aspartic acid; (D) arginine; (E) ornithine, and (F) N-acetylornithine were found in the culture medium. N =3; Y-axis: normalised concentration; intracellular aspartic acid levels were not consistent between positive and negative ion modes

to the incorporation of arginine from the media into VISA cells. A membrane-embedded arginine-ornithine antiporter (ArcD) of the ADI pathway transports extracellular arginine into the cell and exports intra-cellular ornithine into the extracellular environment (Lindgren et al. 2014). This could result in the accumulation of ornithine we observed in the VISA culture media and could be attributed to the exchange of cellular ornithine with extracellular arginine by ArcD. The active breakdown of arginine in VISA via the ADI pathway generates increased levels of ammonia and ATP, and ATP is important for cell wall building (Tan et al. 2017). Citrulline, the substrate for ArcB, was found to be in lower levels in our tested VISA cells, fitting with our hypothesis that arginine catabolism via the ADI pathway is important for VISA development in VISAs of the Mu50 lineage. Of note, intra-cellular arginine was reported to be decreased in VISA strain Q2283

(Gardner et al. 2018), whereas citrulline was found to be increased in VISAs of the SG and JH lineages. While the mutations resulting in Q2283 are unknown, the SG and JH lineages carry *yvqF* mutations (Alexander et al. 2014). The discrepancy between arginine and citrulline levels among the different VISA lineages could potentially be attributed to their genetic differences, as the Mu50 lineage does not carry *yvqF* mutations (Hiramatsu et al. 2014).

The ADI pathway is found widely in microorganisms and may be related to bacterial adaptation in hostile environments. Arginine serves as an alternative energy source for *S. aureus* under anaerobic condition when glucose is depleted (Makhlin et al. 2007). However, this does not seem the case for our study, as the strains we tested were cultured under aerobic conditions. The activation of the ADI pathway in VISAs in our study could be attributed to a disturbance in energy metabolism inside cells, due to mutations in *vraS* and *graR* leading to their VISA phenotypes. The VISA Mu50 has been shown to exhibit a shift in glucose metabolism to support accelerated cell wall synthesis by utilising fructose-6-phosphate to generate glucosamine-6-phosphate (Cui et al. 2000). Glucosamine-6-phosphate is the main precursor of cell wall peptidoglycan, whereas fructose-6-phosphate is derived from glycolysis. Shunting glucose from glycolysis to peptidoglycan biosynthesis would likely disturb energy metabolism in VISAs; therefore, the cell must rely on sources other than glucose in order to survive. Further, elevated ATP levels had been found in VISAs used in our study, suggesting active energy production is occurring in these cells (Tan et al. 2017). Taken together, we suggested that arginine served as an alternative source of energy via the ADI pathway for VISAs of the Mu50 lineage and compensated for the glycolytic shunt due to accelerated cell wall synthesis (Figure 7). As ADI is not found in humans, the pathway should be explored further as a target for antibiotic development.

Due to the small sample size used in this study, only a small number of significantly different metabolites was identified between VISAs and VSSA. Trends in concentration changes of metabolites related to arginine metabolism were observed in the tested strains, but these were not statistically significant. Targeted metabolomics on the ADI pathway will be important to validate the findings of this study in the future.

CONCLUSION

We observed altered levels of metabolites associated with arginine catabolism in VISAs of the Mu50 lineage. Breakdown of arginine via the ADI pathway could be activated by VraSR and GraSR in order to use arginine as an alternative energy source for the VISAs to increase cell wall synthesis. However, findings in this study warrant further investigation, as it remains to be determined whether the ADI pathway is important for the development of other VISA lineages.

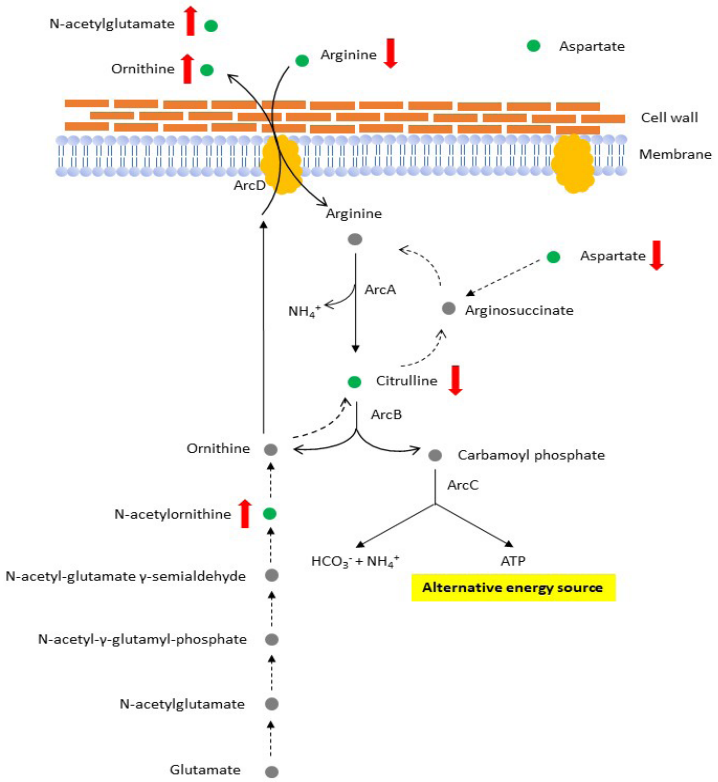

Figure 7: Arginine metabolism in VISA Mu50 lineage. Arginine synthesis pathway is represented by dotted arrows. ADI pathway (arginine catabolism) is represented by solid arrows. Metabolites detected in this study are represented by green circles. Concentration trends of metabolites are represented by red arrows (up: increase; down: de-crease). ArcA: ADI; ArcB: ornithine carbamoyltransferase; ArcC: carbamate kinase; ArcD: arginine-ornithine anti-porter

ACKNOWLEDGEMENT

This research was funded by Ministry of Higher Education (MOHE), Malaysia, through Fundamental Research Grant Scheme under the grant number FRGS/1/2014/SKK04/UKM/03/1. The authors thank Siti Nor Asyikin Zakaria and Geetha Gunasekaran for technical support in mass spectrometry.

REFERENCES

Alexander, E.L., Gardete, S., Bar, H.Y., Wells, M.T., Tomasz, A., Rhee, K.Y. 2014. Intermediate-type vancomycin resistance (VISA) in genetically-distinct *Staphylococcus aureus* isolates is linked to specific, reversible metabolic alterations. *PLoS ONE* **9**(5): e97137.

Chong, J., Soufan, O., Li, C., Caraus, I., Li, S., Bourque, G., Wishart, D.S., Xia, J. 2018. MetaboAnalyst 4.0: Towards more transparent and integrative metabolomics analysis. *Nucleic Acids Res* **46**(W1): W486-94.

Cui, L., Lian, J.Q., Neoh, H.M., Reyes, E., Hiramatsu, K. 2005. DNA microarray-based identification of genes associated with glycopeptide resistance in *Staphylococcus aureus*. *Antimicrob Agents Chemother* **49**(8): 3404-13.

Cui, L., Murakami, H., Kuwahara-Arai, K., Hanaki, H., Hiramatsu, K. 2000. Contribution of a thickened cell wall and its glutamine nonamidated component to the vancomycin resistance expressed by *Staphylococcus aureus* Mu50. *Antimicrob Agents Chemother* **44**(9): 2276-85.

Cui, L., Neoh, H.M., Shoji, M., Hiramatsu, K. 2009. Contribution of vraSR and graSR

point mutations to vancomycin resistance in vancomycin-intermediate *Staphylococcus aureus*. *Antimicrob Agents Chemother* **53**(3): 1231-4.

Dunn, W.B., Broadhurst, D., Begley, P., Zelena, E., Francis-Mcintyre, S., Anderson, N., Brown, M., Knowles, J.D., Halsall, A., Haselden, J. N., Nicholls, A.W., Wilson, I.D., Kell, D.B., Goodacre, R. 2011. Procedures for large-scale metabolic profiling of serum and plasma using gas chromatography and liquid chromatography coupled to mass spectrometry. *Nat Protoc* **6**(7): 1060-83.

Gardner, S.G., Marshall, D.D., Daum, R.S., Powers, R., Somerville, G.A. 2018. Metabolic mitigation of *Staphylococcus aureus* vancomycin intermediate-level susceptibility. *Antimicrob Agents Chemother* **62**(1): e01608-17.

Gil-De-La-Fuente, A., Godzien, J., Saugar, S., Garcia-Carmona, R., Badran, H., Wishart, D.S., Barbas, C., Otero, A. 2019. CEU Mass Mediator 3.0: A Metabolite Annotation Tool. *J Proteome Res* **18**(2): 797-802.

Guijas, C., Montenegro-Burke, J.R., Domingo-Almenara, X., Palermo, A., Warth, B., Hermann, G., Koellensperger, G., Huan, T., Uritboonthai, W., Aisporna, A.E., Wolan, D.W., Spilker, M.E., Benton, H.P., Siuzdak, G. 2018. METLIN: A technology platform for identifying knowns and unknowns. *Anal Chem* **90**(5): 3156-64.

Hattangady, D.S., Singh, A.K., Muthaiyan, A., Jayaswal, R.K., Gustafson, J.E., Ulanov, A.V., Li, Z., Wilkinson, B.J., Pfeltz, R.F. 2015. Genomic, transcriptomic and metabolomic studies of two well-characterized, laboratory-derived vancomycin-intermediate *Staphylococcus aureus* strains derived from the same parent strain. *Antibiotics* **4**(1): 76-112.

Hiramatsu, K., Aritaka, N., Hanaki, H., Kawasaki, S., Hosoda, Y., Hori, S., Fukuchi, Y., Kobayashi, I. 1997. Dissemination in Japanese hospitals of strains of *Staphylococcus aureus* heterogeneously resistant to vancomycin. *Lancet* **350**(9092): 1670-3.

Hiramatsu, K., Kayayama, Y., Matsuo, M., Aiba, Y., Saito, M., Hishinuma, T., Iwamoto, A. 2014. Vancomycin-intermediate resistance in *Staphylococcus aureus*. *JGAR* **2**(4): 213-24.

Kanehisa, M. 2019. Toward understanding the origin and evolution of cellular organisms. *Protein Sci* **28**(11): 1947-51.

Koehl, J.L., Muthaiyan, A., Jayaswal, R.K., Ehlert, K., Labischinski, H., Wilkinson, B.J. 2004. Cell wall composition and decreased autolytic activity and lysostaphin susceptibility of glycopeptide-intermediate *Staphylococcus aureus*. *Antimicrob Agents Chemother* **48**(10): 3749-57.

Kuroda, M., Kuroda, H., Oshima, T., Takeuchi, F., Mori, H., Hiramatsu, K. 2003. Two-component system VraSR positively modulates the regulation of cell-wall biosynthesis pathway in *Staphylococcus aureus*. *Mol Microbiol* 49(3): 807-21.

Liebeke, M., Meyer, H., Donat, S., Ohlsen, K., Lalk, M. 2010. A metabolomic view of *Staphylococcus aureus* and its ser/thr kinase and phosphatase deletion mutants: Involvement in cell wall biosynthesis. *Chem Biol* **17**(8): 820-30.

Lindgren, J.K., Thomas, V.C., Olson, M.E., Chaudhari, S.S., Nuxoll, A.S., Schaeffer, C.R., Lindgren, K.E., Jones, J., Zimmerman, M.C., Dunman, P.M., Bayles, K.W. Fey, P.D. 2014. Arginine deiminase in *Staphylococcus epidermidis* functions to augment biofilm maturation through pH homeostasis. *J Bacteriol* **196**(12): 2277-89.

Makhlin, J., Kofman, T., Borovok, I., Kohler, C., Engelmann, S., Cohen, G. Aharonowitz, Y. 2007. *Staphylococcus aureus* ArcR controls expression of the arginine deiminase operon. *J Bacteriol* **189**(16): 5976-86.

McCallum, N., Karauzum, H., Getzmann, R., Bischoff, M., Majcherczyk, P., Berger-Bächi, B., Landmann, R. 2006. In vivo survival of teicoplanin-resistant *Staphylococcus aureus* and fitness cost of teicoplanin resistance. *Antimicrob Agents Chemother* **50**(7): 2352-60.

McGuinness, W.A., Malachowa, N., DeLeo, F.R. 2017. Vancomycin resistance in *Staphylococcus aureus*. *YJBM* **90**(2): 269-81.

Neoh, H.M., Cui, L., Yuzawa, H., Takeuchi, F., Matsuo, M., Hiramatsu, K. 2008 Mutated response regulator graR is responsible for phenotypic conversion of *Staphylococcus aureus* from heterogeneous vancomycin-intermediate resistance to vancomycin-intermediate resistance. *Antimicrob Agents Chemother* **52**(1): 45-53.

Sumner, L.W., Amberg, A., Barrett, D., Beale, M.H., Beger, R., Daykin, C.A., Fan, T.W.M., Fiehn, O., Goodacre, R., Griffin, J.L., Hankemeier, T., Hardy, N., Harnly, J., Higashi, R., Kopka, J., Lane, A.N., Lindon, J.C., Marriott, P., Nicholls, A.W., Reily, M.D., Thaden, J.J., Viant, M.R. 2007. Proposed minimum reporting standards for chemical analysis. *Metabolomics* **3**(3): 211-21.

Tan, J.K., Zakaria, S.N.A., Gunasekaran, G., Abdul Sani, N.F., Nasaruddin, M.L., Jaafar, F., Abu Bakar, Z.H., Amir Hamzah, A.I.Z., Nor Aripin, K.N., Mohd Rani, M.D., Noh, N. A., Damanhuri, H.A., Mazlan, M., Makpol, S., Wan Ngah, W.Z. 2023. Metabolomics profiling of age-associated metabolites in Malay population. *Oxid Med Cell Longev* **2023**: 4416410.

Tan, X.E., Neoh, H.M., Looi, M.L., Chin, S.F., Cui, L., Hiramatsu, K., Hussin, S., Jamal, R. 2017. Activated ADI pathway: The initiator

of intermediate vancomycin resistance in *Staphylococcus aureus. Can J Microbiol* **63**(3): 260–264.

Tan, X.E., Neoh, H.M., Looi, M.L., Tan, T.L., Hussin, S., Cui, L., Hiramatsu, K., Jamal, R. 2016. Comparative proteomics profiling reveals down-regulation of *Staphylococcus aureus* virulence in achieving intermediate vancomycin resistance. *Malays J Microbiol* **12**(6): 498-505.

Weigel, L.M., Clewell, D.B., Gill, S.R., Clark, N.C., McDougal, L.K., Flannagan, S.E., Kolonay, J.F., Shetty, J., Killgore, G.E., Tenover, F.C. 2003. Genetic analysis of a high-level vancomycin-resistant isolate of *Staphylococcus aureus. Science* **302**(5650): 1569-71.

Wishart, D.S., Feunang, Y.D., Marcu, A., Guo, A.C., Liang, K., Vázquez-Fresno, R., Sajed, T., Johnson, D., Li, C., Karu, N., Sayeeda, Z., Lo, E., Assempour, N., Berjanskii, M., Singhal, S., Arndt, D., Liang, Y., Badran, H., Grant, J., Serra-Cayuela, A., Liu, Y., Mandal, R., Neveu, V., Pon, A., Knox, C., Wilson, M., Manach, C., Scalbert, A. 2018. HMDB 4.0: The human metabolome database for 2018. *Nucleic Acids Res* **46**(D1): D608-17.